SOLAR DOPPLER SHIFTS: SOURCES OF CONTINUOUS SPECTRA

T. L. Duvall, Jr.
Laboratory for Astronomy and Solar Physics
NASA/Goddard Space Flight Center
Greenbelt, Maryland 20771 USA

and

J. W. Harvey
National Solar Observatory
National Optical Astronomy Observatories*
Tucson, Arizona 85726 USA

ABSTRACT. Oscillation observations can be used to study non-oscillatory solar phenomena that exhibit Doppler shifts. In this paper we discuss several effects of these phenomena and their associated temporal and spatial power spectra: 1) They limit the signal-to-noise ratio and sometimes detectability of oscillation modes. 2) There is the potential for better understanding and/or detection of solar phenomena: surface rotation, supergranulation, granulation, active regions, giant cells, and mesogranulation. 3) Large-scale convection may spatially modulate oscillation modes, leading to a continuous background spectrum. 4) In regions of the spectrum where we lack the resolution to separate modes, we can determine upper limits for the integrated effects of modes.

1. INTRODUCTION

Observations of solar oscillations are made in the presence of noise from instrumental, atmospheric and solar sources. This noise limits the accuracy of oscillation mode frequency and amplitude measurements. In this paper we demonstrate how accurate estimates of the precision of mode frequency measurements can be made and outline a method for modelling observed spectra. The solar component of the "noise" provides important information about many solar phenomena. We discuss some of the results from available observations of the background spectrum. The inhomogeneous structure of the convection zone may alter the modal structure of the oscillations in such a way to produce sidebands around modal features in k,ω spectra. We conjecture that such a process may contribute to the rise of background power level in such spectra. Finally, we use results from a 17-day observation sequence to set limits on the

*Operated by the Association of Universities for Research in Astronomy, Inc. under contract with the National Science Foundation.

integrated strength of unresolved g-modes of degree 2.

2. THE EFFECT OF BACKGROUND POWER ON THE S/N RATIO OF OSCILLATION FREQUENCY MEASUREMENTS

It is obvious that sources of background power will limit the accuracy of estimates of oscillation mode frequencies. Here we address the following issues: 1. Quantitatively, how much are the frequencies affected as a function of signal to noise ratio? 2. What is an optimum method for estimating frequencies and their uncertainties? The need for reliable estimates of frequency uncertainties is particularly evident in the inversion calculations, where the uncertainties in the final product (say solar rotation versus depth) are critically dependent on the estimates of internal error in the frequency measurements (Christensen-Dalsgaard and Gough, 1984; Gough, 1984). What we assume in this section is that there are two sources of uncertainty in frequency measurements, one component due to background power and the other due to the stochastic nature of the modes themselves. It is this second source, due basically to the finite lifetimes of the modes, that gives the fundamental limitation of mode frequency measurement. In practice, however, we feel that the observations to date have not approached this fundamental limit but instead are limited by background sources of power.

2.1. A Model of Oscillations and Noise

We will begin the discussion (following Jenkins and Watts, 1968) by considering a simple example of a stochastic process: a harmonic oscillator with damping driven by a random forcing function. The differential equation describing the system is:

$$\frac{1}{\omega_o^2}\frac{d^2y}{dt^2}+\frac{1}{\omega_o Q}\frac{dy}{dt}+y(t)=x(t) \tag{1}$$

where $y(t)$ is the displacement, ω_o is the undamped oscillator frequency, Q is a constant describing the damping, and $x(t)$ is the forcing function. This is an example of an equation (linear differential equation with constant coefficients) whose solution can be expressed as a convolution:

$$y(t)=\int_{-\infty}^{\infty}h(t')x(t-t')dt' \tag{2}$$

The function $h(t)$, called the impulse response of the system, is independent of the forcing function $x(t)$ and so only depends on the left side of equation (1). $h(t)$ must satisfy a condition of physical realizability ($h(t)=0, t<0$) and must be integrable. Using the convolution theorem, the Fourier transform of equation (2) is:

$$\tilde{y}(f)=H(f)\,\tilde{x}(f) \tag{3}$$

where $\tilde{y}$, $\tilde{x}$ are the transforms of $y(t)$, $x(t)$, and $H(f)$ is the transform of $h(t)$ and is termed the frequency response function of the system. To derive the frequency response function for our example of the harmonic oscillator, one would do the Fourier transform of equation (1). And, in fact, $|H(f)|^2$ is what gives our normal Lorentz line shape. It is the parameters describing $|H(f)|^2$ that we would ultimately wish to estimate.

If one computes the power spectrum of a finite realization (of length T) of the $y(t)$ process (we will call this a sample spectrum), one does not obtain $|H(f)|^2$ directly because of the random nature of $\tilde{x}(f)$. Considering the sample spectrum of the $x(t)$ process separately (calling it $C_x^T(f)$), we find that at frequencies separated by $1/T$ the values are independent and distributed as χ^2 with two degrees of freedom. This leads to a definition of the "spectrum" of the $x(t)$ process as:

$$\Gamma_x(f) = \lim_{T\to\infty} E[C_x^T(f)] \tag{4}$$

where the expectation operator, E, implies an average over many independent realizations. For a white noise process, this is just a constant, independent of f (and hence a flat spectrum from white noise). Similarly, the spectrum of the $y(t)$ process is:

$$\Gamma_y(f) = |H(f)|^2 \ \Gamma_x \tag{5}$$

As for the white noise case, the ratio (at a given frequency) of the sample spectrum divided by the true spectrum is distributed as χ^2 with two degrees of freedom. This is used as the basis for a maximum likelihood method for estimation of $\Gamma_y(f)$ given a sample spectrum. That the solar data actually possess this property has been demonstrated by Woodard (1984).

The maximum likelihood technique consists of constructing the joint probability density for the outcome of an experiment in terms of some model parameters. Then maximizing this probability density (or likelihood function) for a given experimental outcome yields the maximum likelihood estimates of the parameters. In the present example, we have at a given frequency f_i, the probability density

$$p(C_i) = \frac{1}{\Gamma_i} \exp(-C_i/\Gamma_i) \tag{6}$$

where we have adopted the simplified notation that C_i, Γ_i are respectively the sample spectrum and the spectrum at frequency f_i. The joint probability density for the experimental outcome at all the independent frequencies is just the product of the individual densities:

$$L = \exp[-\sum_i (\ln\Gamma_i + C_i/\Gamma_i)] \tag{7}$$

The model might be, for example, a sum of Lorentzian plus background power:

$$\Gamma_i = \frac{A}{1 + \left(\frac{f_i - f_o}{w}\right)^2} + r \tag{8}$$

where A is the maximum signal power, w is the half-width and r is the background power. For this case, one takes a given sample spectrum C_i and maximizes equation (7) in terms of the model parameters f_o, A, w, r.

2.2. Fitting Observations and Estimating Uncertainty

The analysis of the uncertainties is most easily done if the likelihood function is approximately Gaussian for variations of the fitting parameters. If it is Gaussian, the likelihood function can be considered equivalent to a probability

density function for the parameters and the error analysis can proceed similarly to that for a normal multiple regression. If it is not Gaussian, it is sometimes possible to change the desired parameters to make it Gaussian. For example, in the case of Lorentzian plus background we found in simulations that if the likelihood function was expressed in terms of the logarithms of the parameters A,w,r, that it was approximately Gaussian.

To test the fitting procedure and error estimation, a series of simulations was performed on the model of Lorentzian plus background. In all cases, the resolution used was that of the 1980 ACRIM data: 1/290 days = 0.04 μHz and the FWHM of the modes was 1.6 μHz.

Sample spectra were generated at this resolution over a range of ± 10 μHz from a mode position for four different values of the peak signal to background ratio (A/r). Fifty realizations were computed for each value of A/r under the assumption that the ratio of sample spectrum to model should be distributed as χ^2 with two degrees of freedom. To check the error estimation procedure, the internal error estimates were averaged over the 50 cases and compared to the external scatter found in the parameters. This comparison showed that the internal error estimates are in fact good estimates of the parameter uncertainties.

The critical parameter is the frequency estimation error and the results of the simulations are shown in Fig. 1 and Table 1. The results are presented in the figure as σ^2 (variance of frequency estimate) versus r/A in order to show the linear relationship between these two variables.

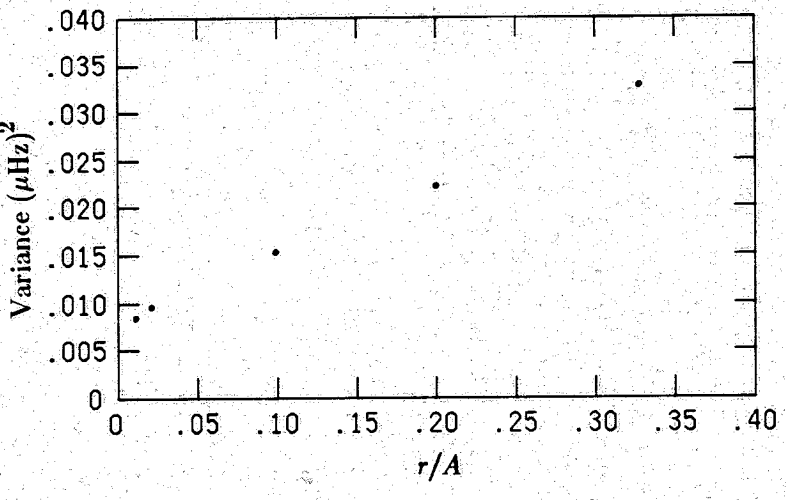

Figure 1. The mean uncertainty squared (variance) of frequency estimates as a function of background noise level divided by peak signal power for the simulations discussed in the text. Note the linear trend.

One sees that measurement uncertainty decreases as S/N ratio increases, as expected. However, even for infinite S/N ratio, a finite measurement error remains. This is partly due to the finite mode lifetime and also partly due to only using the data $\pm 10\mu$Hz around the mode. One rather disappointing aspect of this plot is the rather slow decrease of measurement error for substantial increases of S/N ratio.

TABLE I. Simulation results

A/r	3	5	10	50	100
σ (μHz)	0.181	0.149	0.124	0.098	0.092

3. DETECTION OF SURFACE PHENOMENA -- THE SOLAR BACKGROUND SPECTRUM

The other solar surface phenomena (besides oscillations) that contribute to Doppler-shift observations are rotation, limb effect, gravitational redshift, supergranulation, active regions, granulation, giant cells and mesogranulation. All of these phenomena are impediments to observing oscillations, but we may be able to learn something about these phenomena from oscillation observations. For example, one might like to know what is the spatio-temporal power spectrum of supergranulation. Phrased in this way, the question is very difficult to answer: all of the phenomena are lumped together and it will be nontrivial to separate them. A more reasonable question might be: what is the spatio-temporal power spectrum of solar non-oscillatory Doppler shifts? As we shall see, this also is not an easy question to answer.

What do we expect for the spatio-temporal power spectra? We can get some guidance from a simple model given by Harvey (1985) for the lowest spatial frequencies. In this model each solar phenomenon is described by an exponentially decaying in time, autocovariance function. This leads to a Lorentzian-shaped temporal power spectrum (centered at ν=0). Each of the different phenomena has its own lifetime and amplitude. The proposed temporal power spectrum for integrated sunlight is shown in Fig. 2. The steep falloff with frequency is due to the ν^{-2} wings of the Lorentz profile. The spectrum is not expected to change significantly up to spherical harmonic degree of roughly 50.

There are a number of observational difficulties with measuring the spatio-temporal power spectrum of the non-oscillatory Doppler shifts. The power spectrum of the temporal window function for a completely sampled interval falls off as ν^{-2}. Thus, even if signals were only present at low frequencies, the resulting spectrum would appear similar to Fig. 2 because of leakage. This could be cured by apodization for a completely sampled sequence. However, for a sequence with significant data gaps the problem is more severe. In general, the spectrum of the window function falls off more slowly than ν^{-2} and is not as easily corrected by apodization.

Another severe problem at least at higher spatial frequencies is heterodyning of the low frequency signal (mostly supergranulation and active regions) by the atmospheric seeing (Ulrich *et al.* 1984). As the seeing is generally at a higher frequency than the sampling, the result is a roughly flat background spectrum (Hill, 1984). This background may be the dominant signal at higher spatial frequencies and many temporal frequencies. This would prevent the measurement of the solar background spectrum in these areas. It is also a severe impediment for oscillation observations. The amount of "homogenizing" of the temporal spectrum will change as a function of spatial frequency, making the variation of solar power with spatial frequency uncertain. Another source of uncertainty of variations with spatial frequency is the instrumental point-spread function, which needs to be measured. Potentially severe problems at all spatial frequencies are purely instrumental sources of noise increasing at low frequencies. The

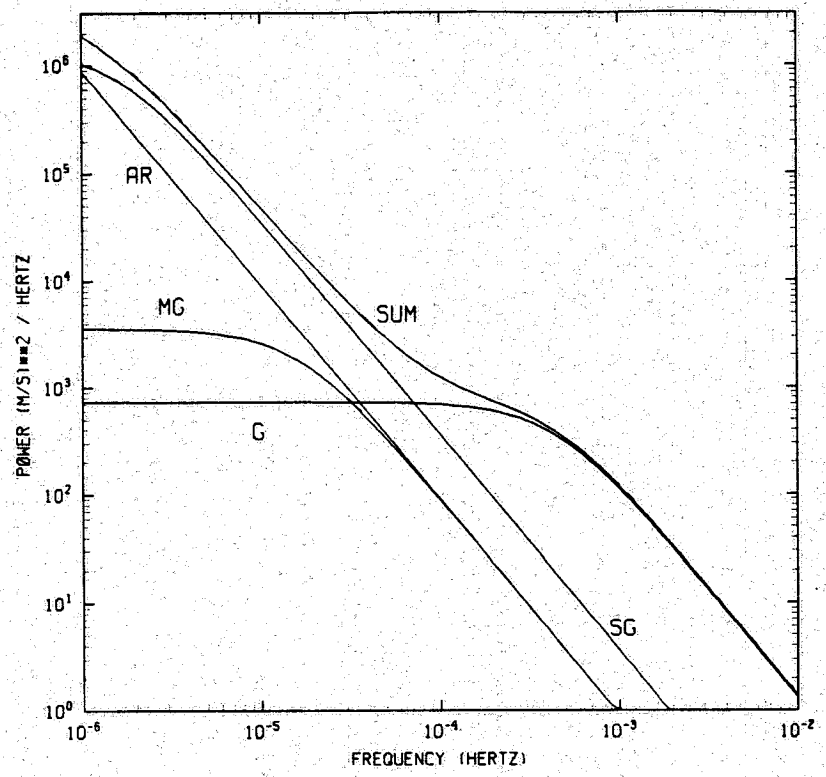

Figure 2. The model power spectrum for integrated sun observations. The curve labelled SUM is the sum of the spectra for the individual physical processes (shown separately) : AR (active regions), SG (supergranulation), G (granulation), and MG (mesogranulation).

spectra of such noise sources are almost never known accurately and can be difficult to separate from solar phenomena, although sometimes solar rotation can be used to provide a means of discrimination.

Given these uncertainties, what can be learned about the background spectrum from present observations? One good data set to examine is the 17-day sequence of sectoral mode observations described by Duvall and Harvey (1984). In Fig. 3 is shown a low-pass (temporally) filtered picture of the data. The dominant signal is solar, as evidenced by the rotation across the disk of almost all visible features. The picture would appear to be dominated by active region signals and a signal showing horizontal motion. The active region signal is manifested as apparent recession (white) most strongly visible near disk center. The most obvious of these features have been identified with particular active regions rotating across the disk. The horizontal motion signal, probably supergranulation but possibly also giant cells, is of generally higher spatial frequency and visible mostly away from the disk center.

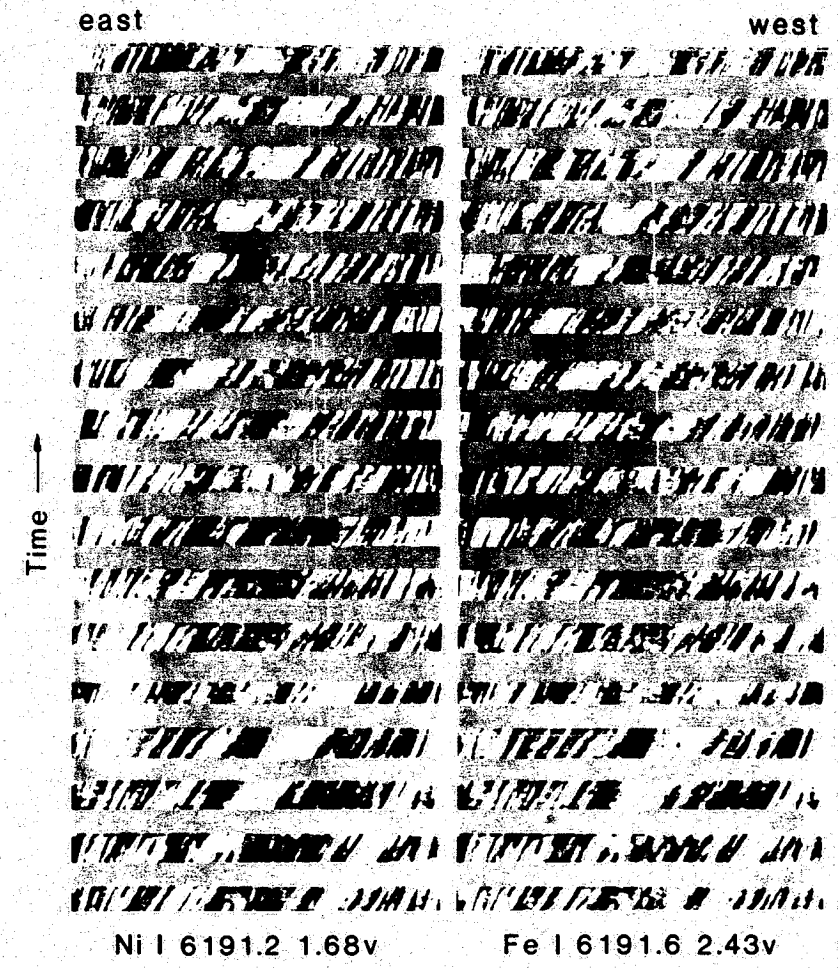

Figure 3. Low-pass filtered Doppler shift versus time for the data of Duvall and Harvey (1984). The two pictures are for the two spectrum lines used. Time proceeds upwards for 17 days. Space goes horizontally, east limb to west limb. White corresponds to apparent recession. Features do not move in straight lines because we are observing the surface of a sphere projected onto a disk.

The spatial-temporal power spectrum of the low frequency data is shown in Fig. 4. This picture is dominated by the rotating pattern of Fig. 3, which appears as an apparent prograde sectoral ridge with frequency $l\Omega$, l being the spherical harmonic degree, Ω the cyclic rotation frequency. The sideband structure of this feature associated with the nightly gaps is generally the strongest thing seen at frequencies separated by ≥ 10 μHz from $l\Omega$. So we conclude that, without a more detailed analysis, the only definitely solar signal is within a few μHz of $l\Omega$. A marked feature is the strong falloff of the power at high degree. This could be attributed to the instrumental point spread function, as we do not have a good measure of it for these observations. We notice that at higher degrees, the rotational feature is somewhat broader, suggesting a positive correlation of lifetime with feature sizes. Such a correlation was also seen in the supergranulation observations of Duvall (1980). Another noticeable feature is an enhancement of

power near degree = 40. This relatively narrow feature in l is at a size scale about three times larger than supergranulation and is of unknown origin. We unsuccessfully sought a corresponding feature in the sectoral harmonic spectrum of magnetic field patterns observed at the same time as the Doppler measurements. This feature is better seen in Fig. 5, a plot of the integrated power ±5 μHz about the frequency of $l\Omega$. The low frequency results shown in Figs. 4 and 5 are about the only solid information we can currently get from these data about the solar background.

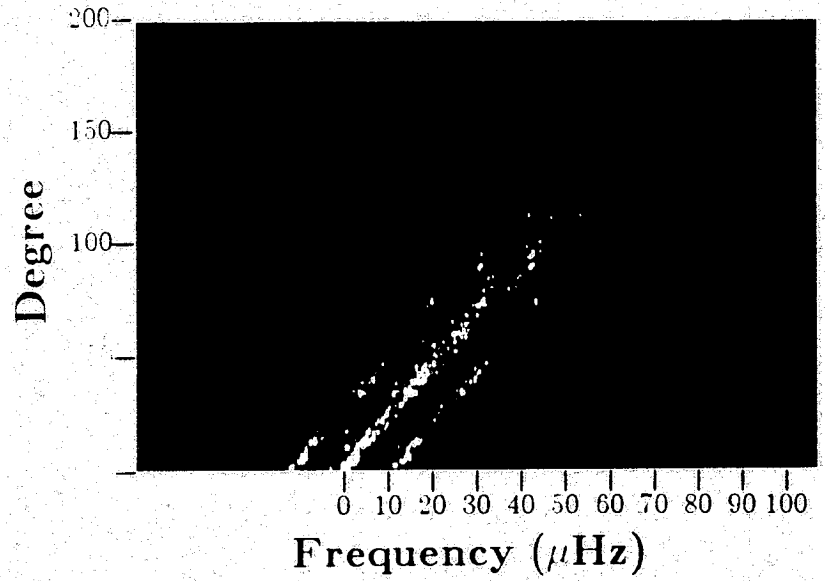

Figure 4. The spatio-temporal power spectrum of Fig. 3. The ordinate is spherical harmonic degree and the abscissa is temporal frequency with waves propagating in the direction of rotation having positive frequency. The central ridge is due to the approximately steady features moving across Fig. 3. The sideband structure is due to the nightly gaps.

A plot of observed power at higher frequencies is shown in Fig. 6. For the reasons discussed above we cannot be certain that the background power observed at higher frequencies is entirely of solar origin. Nevertheless, a comparison of the results of Fig. 6 with the model estimate in Fig. 2 is interesting. The agreement is very good which suggests that either the observations are revealing the true solar background noise or that the simple model estimate seriously overestimates the amount of background power to be expected.

4. A PROPOSED EFFECT OF LARGE-SCALE CONVECTION ON OSCILLATIONS

Helioseismology observations of the inhomogeneities in the Sun due to convection promise the first opportunity for a comprehensive study of astrophysical convection. Convection's effect on the oscillation modes should provide a means for detection of the convective inhomogeneities. The initial attempts to exploit this possibility (Hill, Toomre, and November, 1982, 1983; Gough and Toomre, 1983; Hill, Gough, and Toomre, 1984) have focused on the largest scales of

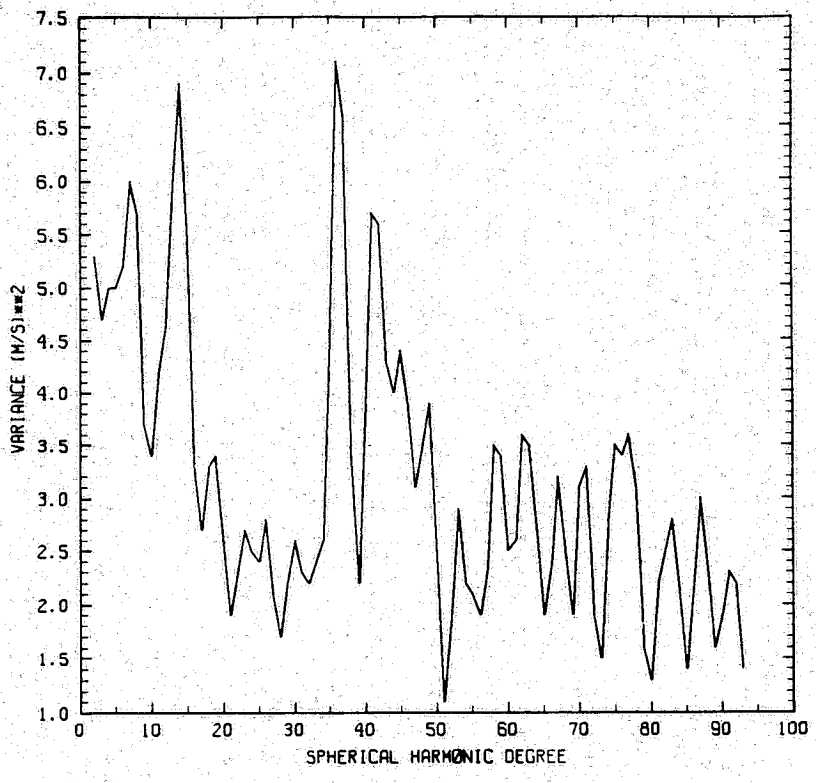

Figure 5. The integrated power over a band ± 5 μHz centered on the frequency $l\Omega$ as a function of spherical harmonic degree.

convection. Searches have been made for variations (from day to day) in advection and frequency for high-degree sectoral modes observed over a large longitude range ($\sim 1/6$ of the solar circumference). The limitation to the largest scales comes from the large longitude range observed: a convective inhomogeneity with more than one wavelength within the observing aperture will effectively be filtered out by the above procedures. The present contribution is concerned with the observation of these higher wavenumber convective inhomogeneities.

The eigenfunction of an oscillation mode for a spherically symmetric system is of the form:

$$E_S = V(r)P_{lm}(\theta)\exp[i(m\phi+\omega t)] \tag{9}$$

For a nonspherical system with a convective perturbation which is sinusoidal in longitude and long-lived, modes will still exist with a well-defined frequency. However, their spatial eigenfunction will be modified. One possibility for this modification is that the horizontal spatial frequency will be modulated, an analogy being an FM radio signal. The form of the eigenfunction in this case would be:

$$E_N = V(r)P_{lm}(\theta)\exp[i(m\phi+a\sin n\phi+\omega t)] \tag{10}$$

where n is the wavenumber of the convection and a is a constant measuring the strength of interaction. This type of relation is normally considered only in the case $n<<m$. Another possibility is that the mode would be amplitude modulated

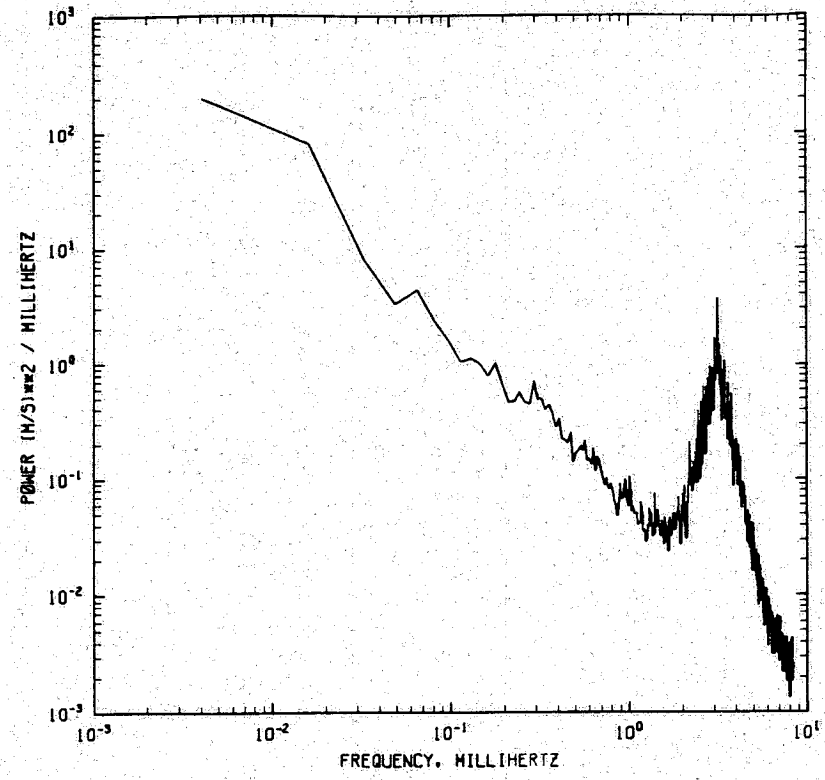

Figure 6. Power spectrum of Doppler shifts for spherical harmonic degree 15. The resolution has been reduced by piece-wise integration. Comparison with the model of Fig. 2 shows good agreement.

in longitude, with the result in the spectrum being qualitatively similar for weak FM modulation.

For the case in which the convective perturbation is resolved in longitude, the spectrum of eq. (10) consists of a carrier and sideband structure. The carrier appears at (m,ω) and for weak modulation, a single pair of sidebands appear at $(m\pm n,\omega)$. Except for edge effects, this spectrum would be constant from day to day, in contrast to the case in which the convective mode is not resolved spatially. For fairly high wavenumber convection (e.g. n=40), the effect of the convection (the sidebands) appears far from the normal mode frequency. And, in fact, if we expect a continuous spectrum of convection, there should be generated a continuous background in the oscillation spectrum which has a higher amplitude at temporal frequencies where the oscillation power is high.

This excess background is one potentially observable effect of the convection. To look for this effect, we have examined the data of Duvall and Harvey (1984). Fig. 7 is a plot of the degree = 150 spectrum at reduced temporal frequency resolution. There is an excess of background power between the mode peaks, amounting to about 2% of the peak oscillation power. However, until a more detailed analysis can be done to decide whether this could be due to the finite extent of the spectrum of the window function, this can only be considered an upper limit to the magnitude of the effect.

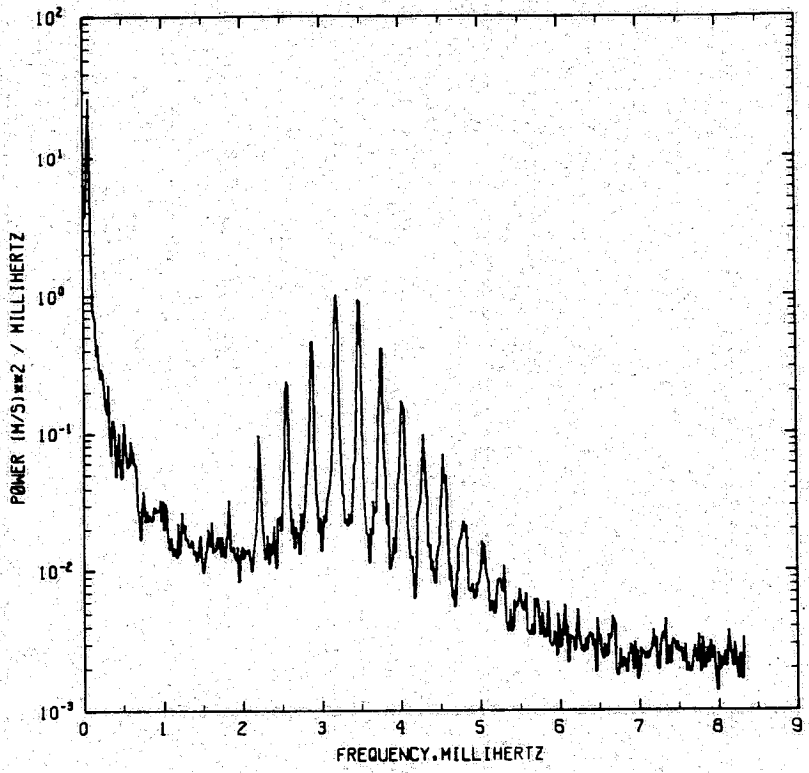

Figure 7. Power spectrum for degree 150. Note the rise in background power between the peaks.

5. UPPER LIMITS TO MODE AMPLITUDES IN UNRESOLVED REGIONS OF THE SPECTRUM

There has been much interest recently in the detection of g-modes because of the diagnostic capabilities of these modes. One contribution that low temporal-resolution observations can make is to set upper limits on the integrated modal power. For example, from Fig. 5, we can state that the upper limit of the integrated power of g-modes of degree = 2 in the frequency band $\pm 5\mu$Hz centered on $l\Omega$ is ~ 5 (m/s)^2. At first sight this might not seem to be a stringent upper limit, but there are a lot of modes in this frequency band and so the mean power per mode must be small. The asymptotic formulas suggest that there would be an infinite number of modes in this frequency band or about 1700 in the band 1-5μHz.

6. CONCLUSIONS

A study of a reasonable model of a solar oscillation mode in the presence of background noise shows that at low signal-to-noise ratio, background noise is a serious source of uncertainty in making estimates of the frequencies of oscillation modes. The reduction of this uncertainty with increasing signal-to-noise ratio is disappointingly slow because of the intrinsic finite lifetime of the modes.

Comparison of a model of solar non-oscillatory power with observations gives good results at high frequencies but there are many uncertainties that prevent us from learning more about solar phenomena from this comparison. Future observations with better equipment and smaller window-function sidelobes should allow considerable information about surface velocity patterns to be reliably obtained. In the meantime, available observations of the spatial spectrum below a frequency of 5μHz suggest that a velocity pattern having a degree of about 40 is a significant solar feature. The same observations indicate that the integrated power from g modes at low frequency is small.

We conjecture that small-scale convection may modulate the pattern of oscillation modes so as to spread power rather far from its origin in k,ω spectra. If proven to be true, this phenomenon is both a nuisance because it adds to the background noise but is also a potential diagnostic of some of the properties of solar convection.

7. REFERENCES

Christensen-Dalsgaard, J. and Gough, D. O.: 1984, in R. K. Ulrich (ed.) *Solar Seismology from Space* (Jet Propulsion Laboratory Publication 84-84, Pasadena) p. 79.

Duvall, T. L., Jr.: 1980, *Solar Physics* **66**, 213.

Duvall, T. L., Jr., and Harvey, J. W.: 1984, *Nature* **310**, 19.

Gough, D. O.: 1984, in R. K. Ulrich (ed.) *Solar Seismology from Space* (Jet Propulsion Laboratory Publication 84-84, Pasadena) p. 49.

Gough, D. and Toomre, J.: 1983, *Solar Physics* **82**, 401.

Harvey, J.: 1985, in E. Rolfe and B. Battrick (eds.) *Future Missions in Solar , Heliospheric, & Space Plasma Physics* (ESA SP-233, European Space Agency, Noordwijk) p.199.

Hill, F.: 1984, in R. K. Ulrich (ed.) *Solar Seismology from Space* (Jet Propulsion Laboratory Publication 84-84, Pasadena) p. 255.

Hill, F., Toomre, J. and November, L. J.: 1982, in J. P. Cox and C. J. Hansen (eds.) *Pulsations in Classical and Cataclysmic Variable Stars* (Joint Institute for Laboratory Astrophysics, Boulder) p. 139.

Hill, F., Gough, D. and Toomre, J.: 1984, *Mem. Soc. Astron. Ital.* **55**, 153.

Hill, F., Toomre, J. and November, L. J.: 1983, *Solar Physics* **82**, 411.

Jenkins, G. M. and Watts, D. G.: 1968, *Spectral Analysis and its Applications*, Holden-Day, San Francisco.

Ulrich, R. K., Rhodes, E. J., Jr., Cacciani, A. and Tomczyk, S.: 1984, in R. K. Ulrich (ed.) *Solar Seismology from Space* (Jet Propulsion Laboratory Publication

84-84, Pasadena) p. 263.

Woodard, M.: 1984, Ph.D. Thesis, University of California, San Diego, Dept. of Physics.